# Supporting Information

# Hydroxy Acid-Functionalized Ionic Liquids as Green Alternatives for Carbonate Synthesis from Carbon Dioxide and Epoxide: Catalytic and Kinetic Investigation

*Shuang Yue*[a], Xuejuan Wang[a], Yuee Wu[a], Sining Zhang[a]*

*Institute of Rare and Scattered Elements Chemistry, College of Chemistry, Liaoning University, Shenyang, Liaoning 110036, China*

## Characteristic data:

**Ionic liquid 1**:

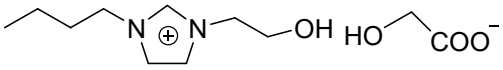


(1) [HEBim][GA]

$C_{11}H_{20}N_2O_4$(244). $^1$H NMR ($D_2O$, 300 MHz) δ：7.49 (s, 2H), 4.32 – 4.25 (m, 2H), 4.18 (t, J = 7.1 Hz, 2H), 3.89 (s, 4H), 1.89 – 1.76 (m, 2H), 1.29 (d, J = 7.6 Hz, 2H), 0.89 (t, J = 7.4 Hz, 3H); $^{13}$C NMR (75.5 MHz, $D_2O$) δ=12.84, 18.91, 31.36, 49.45, 51.66, 59.84, 61.38, 122.49, 122.61, 135.81, 179.49; IR (KBr) ν: 646, 754, 1076, 1165, 1360, 1567, 1606, 1747, 2874, 2960, 3335 $cm^{-1}$.

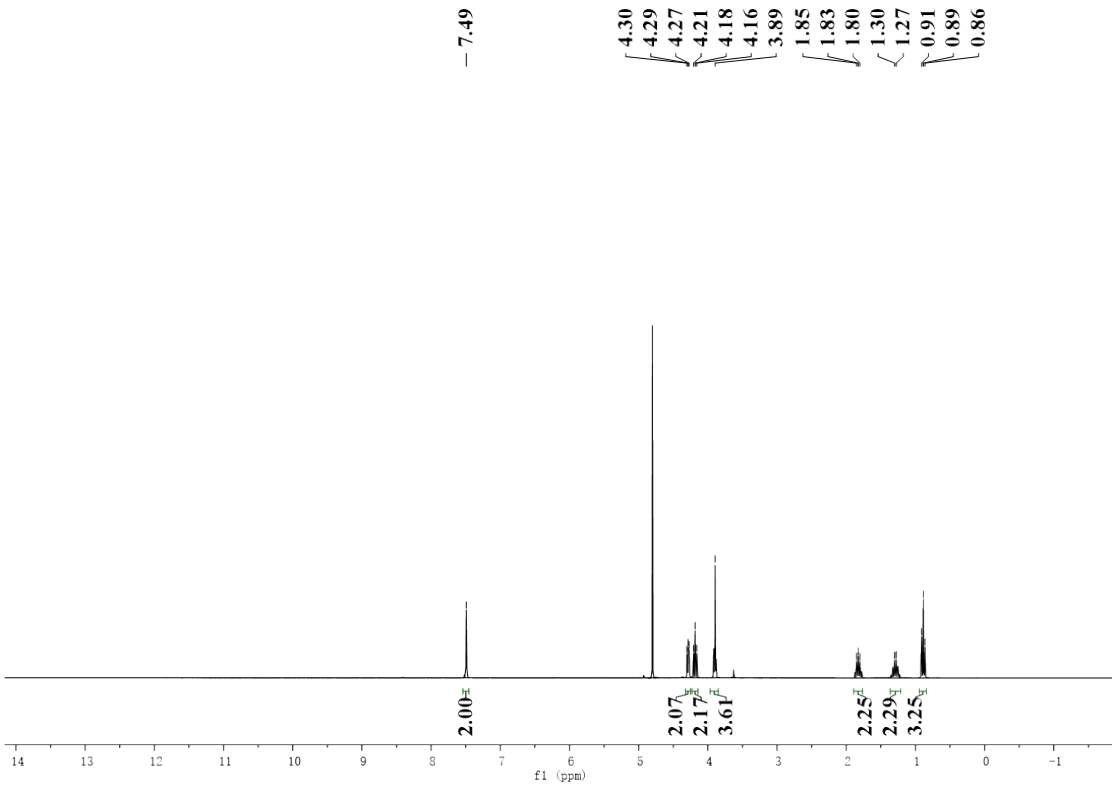


**Figure S1-1.** $^{1}$H NMR spectrum of IL **1.**

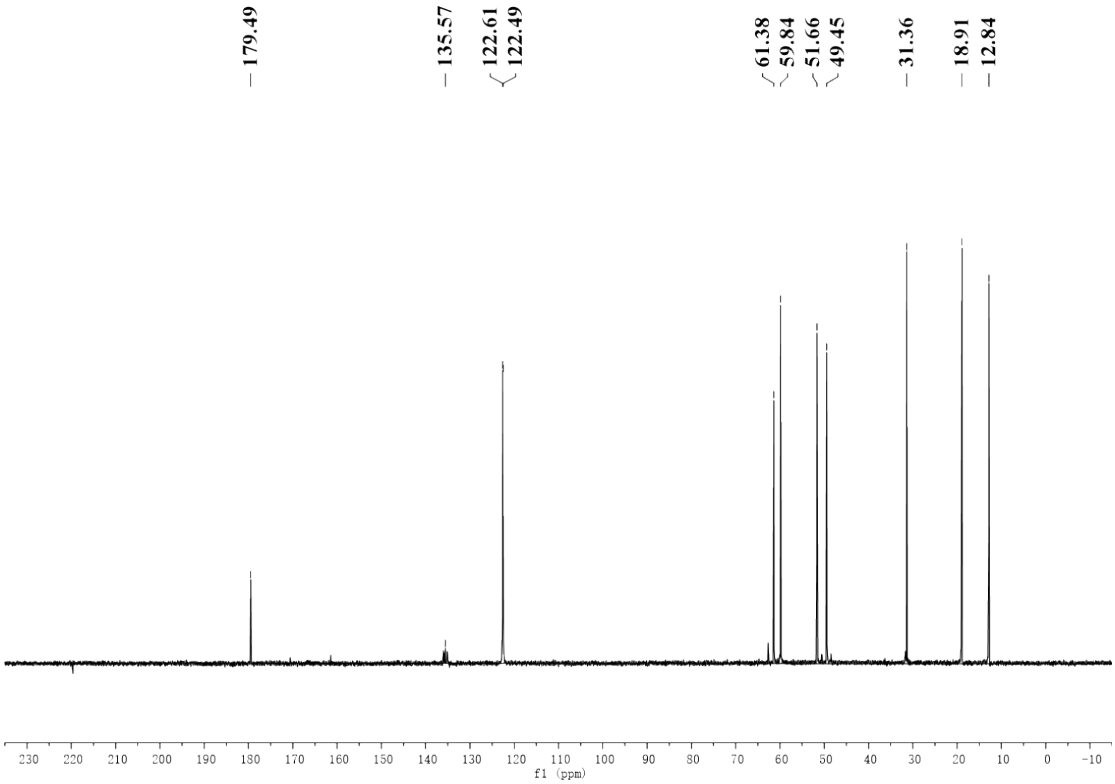


**Figure S1-2.** $^{13}$C NMR spectrum of IL **1.**

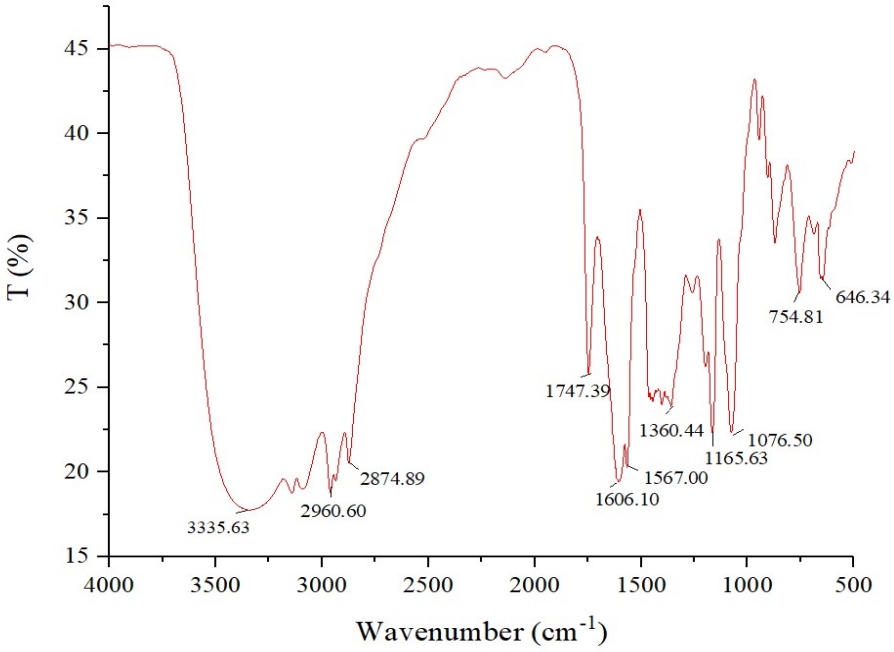


**Figure S1-3.** IR spectrum of IL **1.**

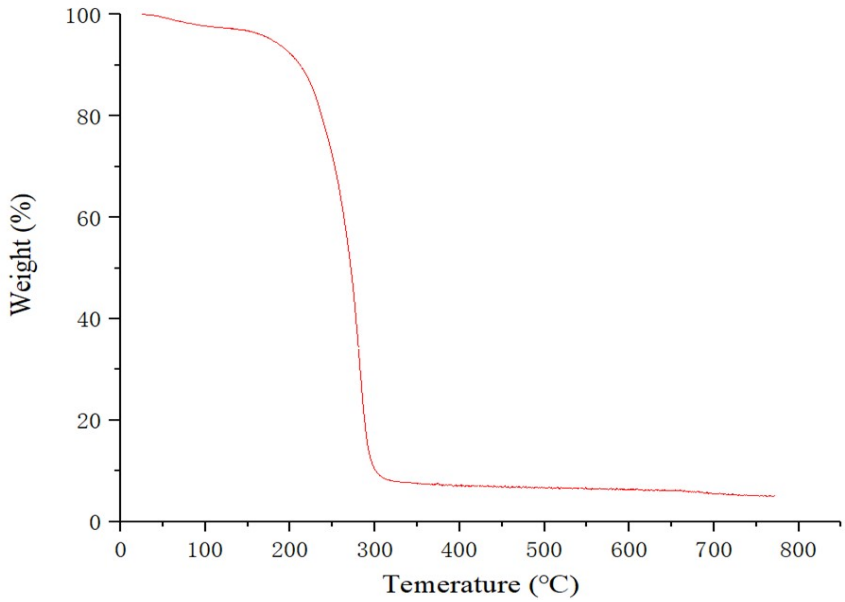


**Figure S1-4.** Degradation of [HEBim][GA] measured by temperature-ramped TGA (10 K/min, 25-800 °C, $N_2$ flow).

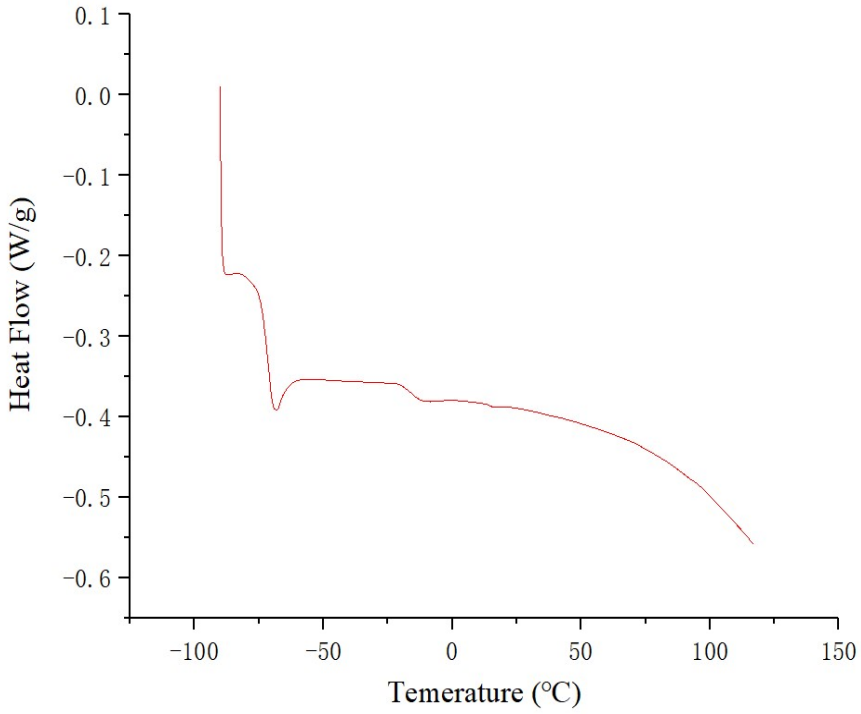


**Figure S1-5.** Differential scanning calorimetry (DSC) analysis of synthesized [HEBim][GA].

**Ionic liquid 2**:

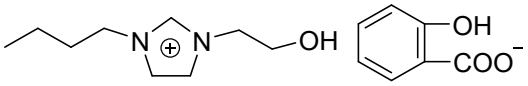


(2) [HEBim][SA]

$C_{16}H_{22}N_2O_4$(306). $^1$H NMR ($D_2O$, 300 MHz) δ: 8.69 (s, 1H), 7.74 (dd, J = 7.8, 1.7 Hz, 1H), 7.48 – 7.29 (m, 3H), 6.96 – 6.81 (m, 2H), 4.26 – 4.19 (m, 2H), 4.08 (t, J = 7.2 Hz, 2H), 3.92 – 3.82 (m, 2H), 1.82 – 1.66 (m, 2H), 1.23 (dd, J = 15.1, 7.5 Hz, 2H), 0.85 (t, J = 7.4 Hz, 3H); $^{13}$C NMR (75.5 MHz, $D_2O$) δ: 12.67, 18.77, 31.01, 49.12, 51.49, 59.58, 116.12, 117.47, 118.88, 121.99, 122.36, 130.34, 133.72, 135.09, 160.06, 174.21; IR (KBr) ν: 665, 762, 1079, 1165, 1384, 1487, 1579, 1633, 2961, 3390 $cm^{-1}$.

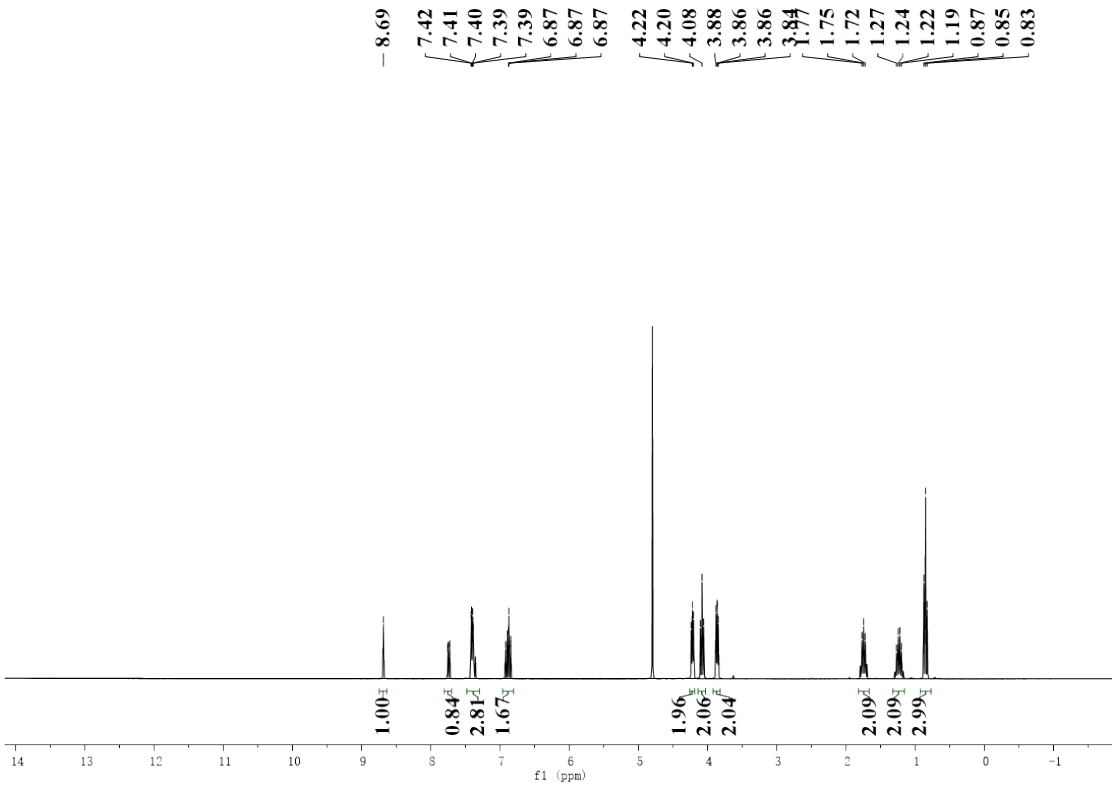


**Figure S2-1.** $^{1}$H NMR spectrum of IL **2.**

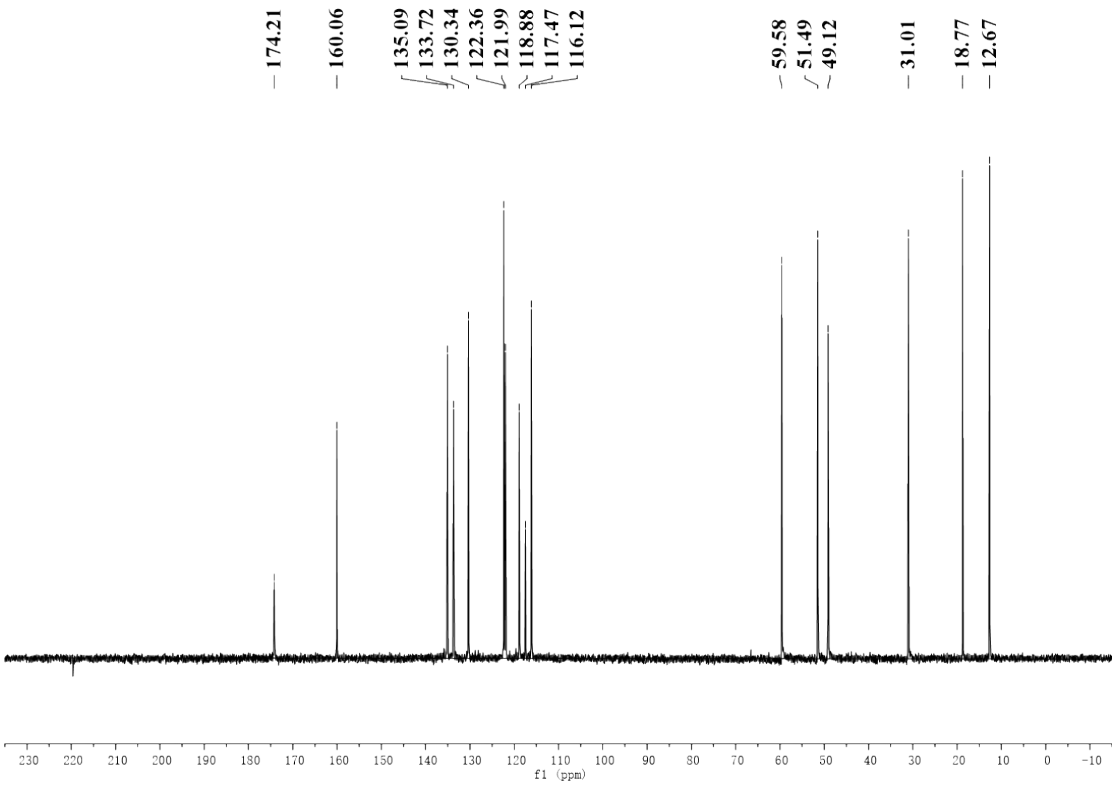


**Figure S2-2.** $^{13}$C NMR spectrum of IL **2.**

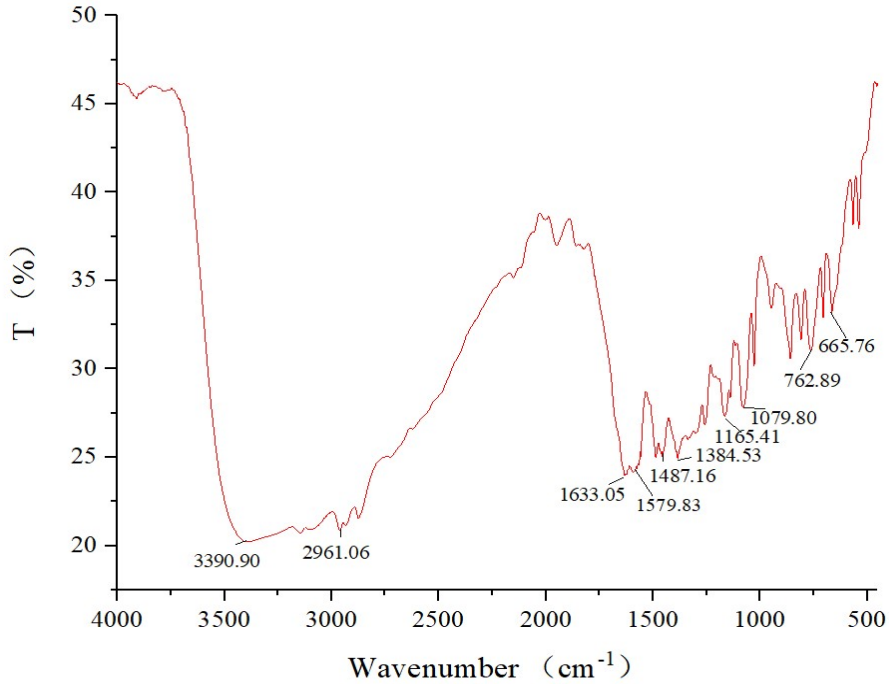


**Figure S2-3.** IR spectrum of IL **2.**

**Ionic liquid 3**:

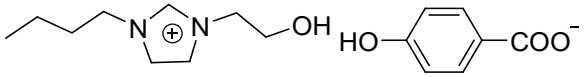


(3) [HEBim][HBA]

$C_{16}H_{22}N_2O_4$(306). $^1$H NMR ($D_2O$, 300 MHz) δ: 7.73 (d, J = 8.8 Hz, 2H), 7.41 (d, J = 3.9 Hz, 2H), 6.80 (d, J = 8.8 Hz, 2H), 4.25 – 4.19 (m, 2H), 4.09 (t, J = 7.2 Hz, 2H), 3.89 – 3.83 (m, 2H), 1.81 – 1.69 (m, 2H), 1.24 (dd, J = 15.1, 7.5 Hz, 2H), 0.85 (t, J = 7.4 Hz, 3H); $^{13}$C NMR (75.5 MHz, $D_2O$) δ: 12.71, 18.82, 31.14, 49.29, 51.51, 59.71, 115.26, 122.26, 122.38, 127.26, 131.34, 135.14, 160.25, 174.84; IR (KBr) ν: 618, 639, 789, 854, 1074, 1163, 1248, 1372, 1551, 1601, 2960, 3387 $cm^{-1}$.

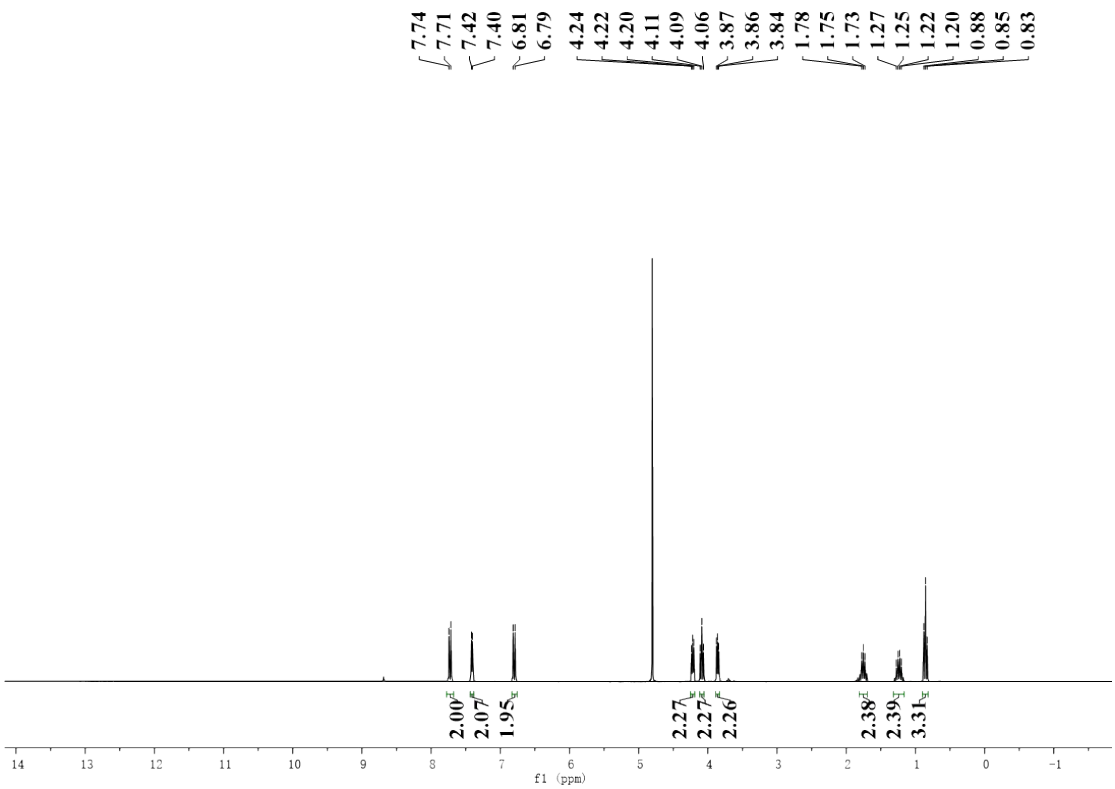


**Figure S3-1.** $^{1}$H NMR spectrum of IL **3.**

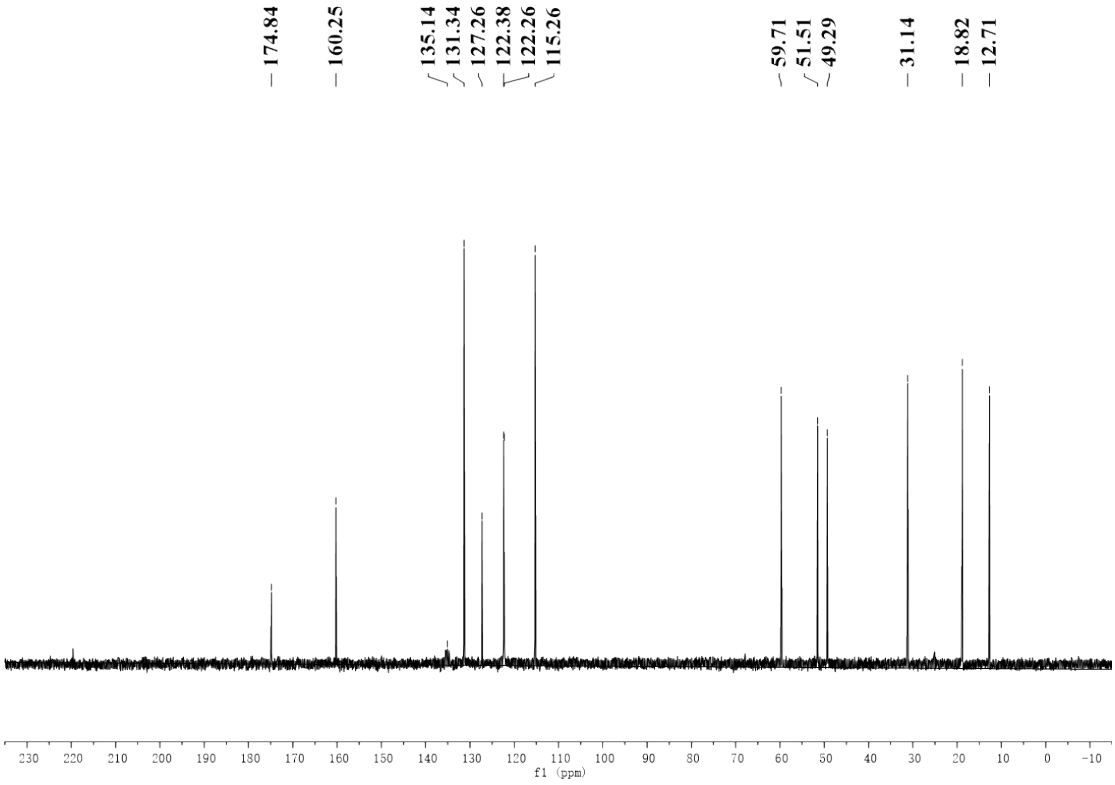


**Figure S3-2.** $^{13}$C NMR spectrum of IL **3.**

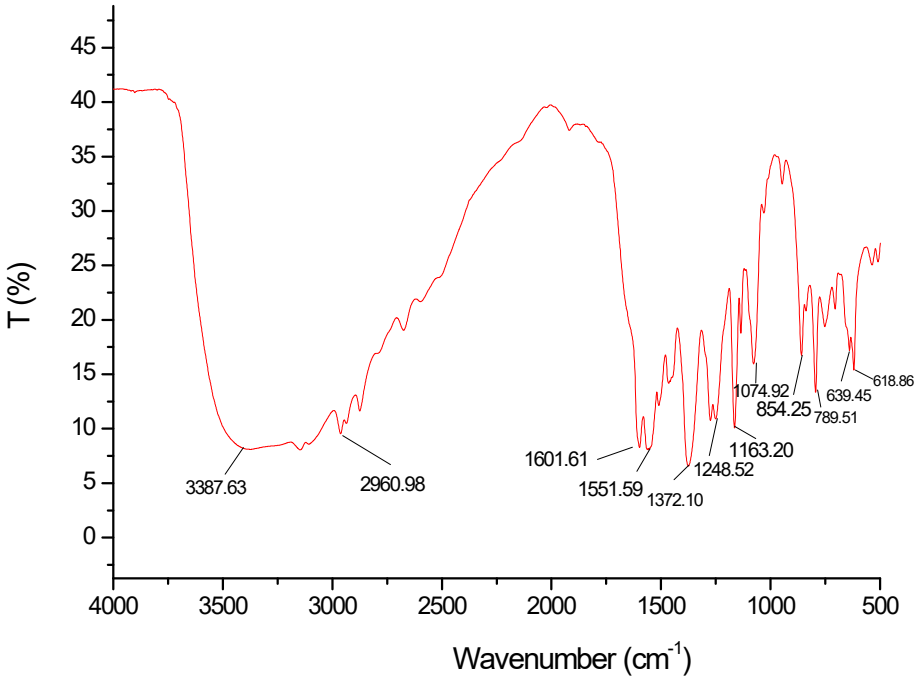


**Figure S3-3.** IR spectrum of IL **3.**

**Ionic liquid 4**:

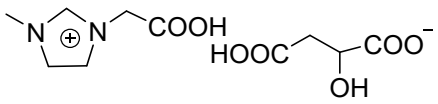


(4) [CEMim][MA]

$C_{10}H_{14}N_2O_4$(274). $^1$H NMR ($D_2O$, 300 MHz) δ: 8.66 (s, 1H), 7.38 (s, 2H), 4.78 (s, 2H), 4.43 (ddd, J = 7.3, 4.4, 1.0 Hz, 1H), 3.87 (s, 3H), 2.76 (dddd, J = 16.3, 8.5, 5.9, 1.1 Hz, 2H); $^{13}$C NMR (75.5 MHz, $D_2O$) δ: 35.81, 39.09, 51.69, 67.49, 123.27, 123.42, 136.99, 172.10, 175.04, 177.50; IR (KBr) ν: 626, 787, 1079, 1176, 1383, 1590, 1720, 1951, 2953, 3151, 3399 cm$^{-1}$.

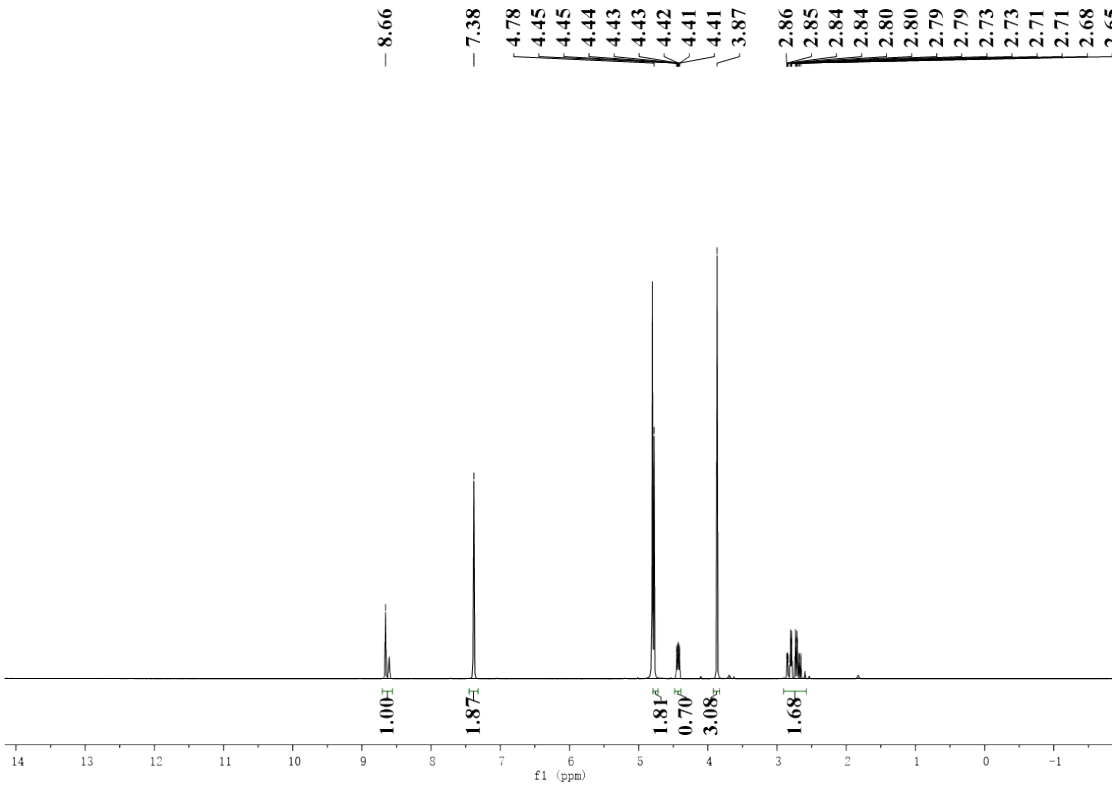


**Figure S4-1.** $^{1}H$ NMR spectrum of IL **4.**

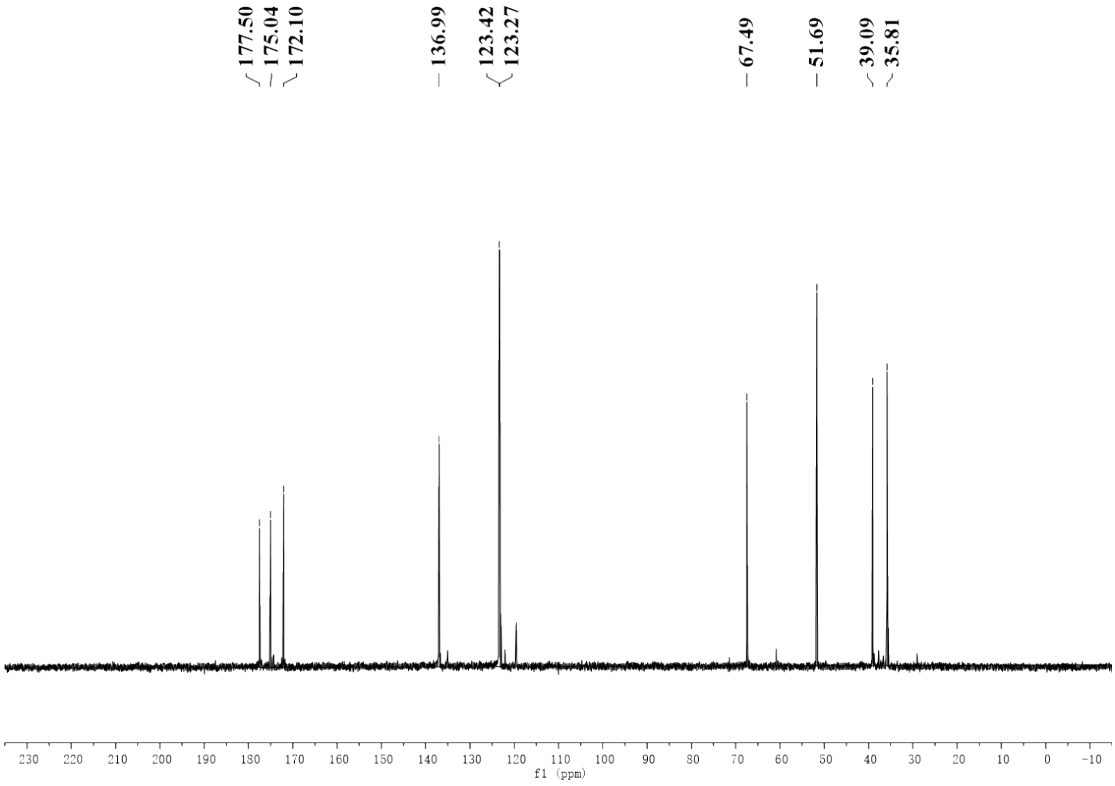


**Figure S4-2.** $^{13}C$ NMR spectrum of IL **4.**

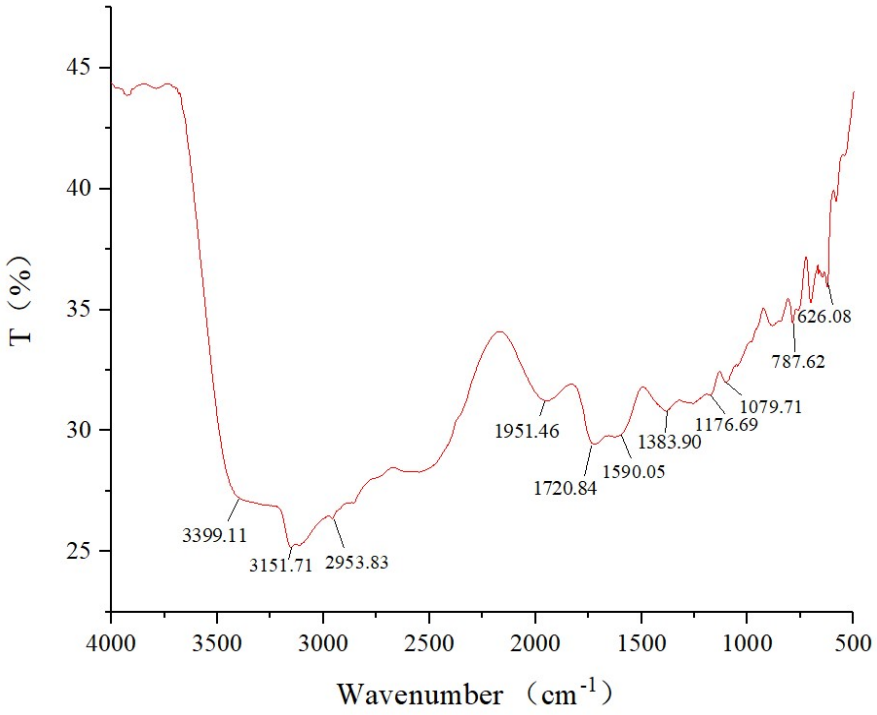


**Figure S4-3.** IR spectrum of IL **4.**

**Ionic liquid 5**:

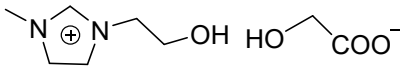


(5) [HEMim][GA]

$C_8H_{14}N_2O_4$(202). $^1$H NMR ($D_2O$, 300 MHz) δ: 8.76 (s, 1H), 7.57 – 7.40 (m, 2H), 4.35 – 4.28 (m, 2H), 3.93 (d, J = 6.6 Hz, 4H), 3.91 (s, 3H); $^{13}$C NMR (75.5 MHz, $D_2O$) δ: 35.84, 51.66, 59.86, 61.32, 122.54, 123.69, 136.50, 179.65; IR (KBr) ν: 646, 754, 1076, 1165, 1360, 1567, 1606, 1747, 2874, 2960, 3335 $cm^{-1}$.

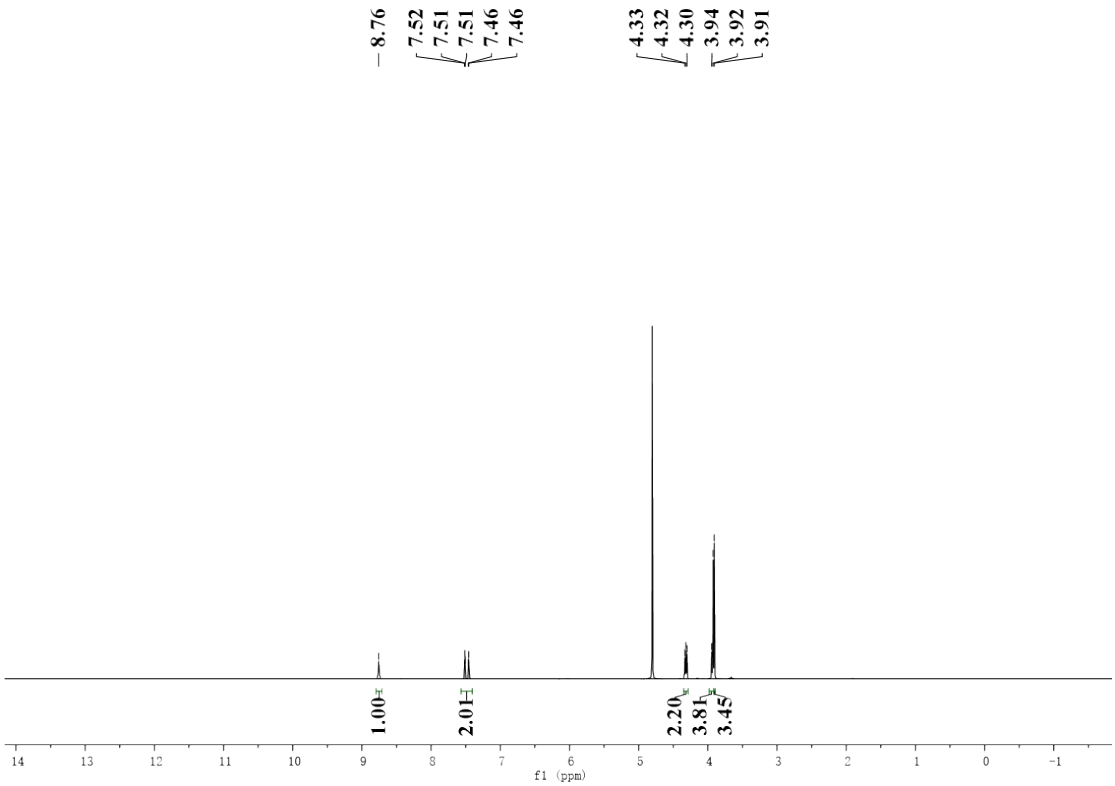


**Figure S5-1.** $^{1}$H NMR spectrum of IL **5.**

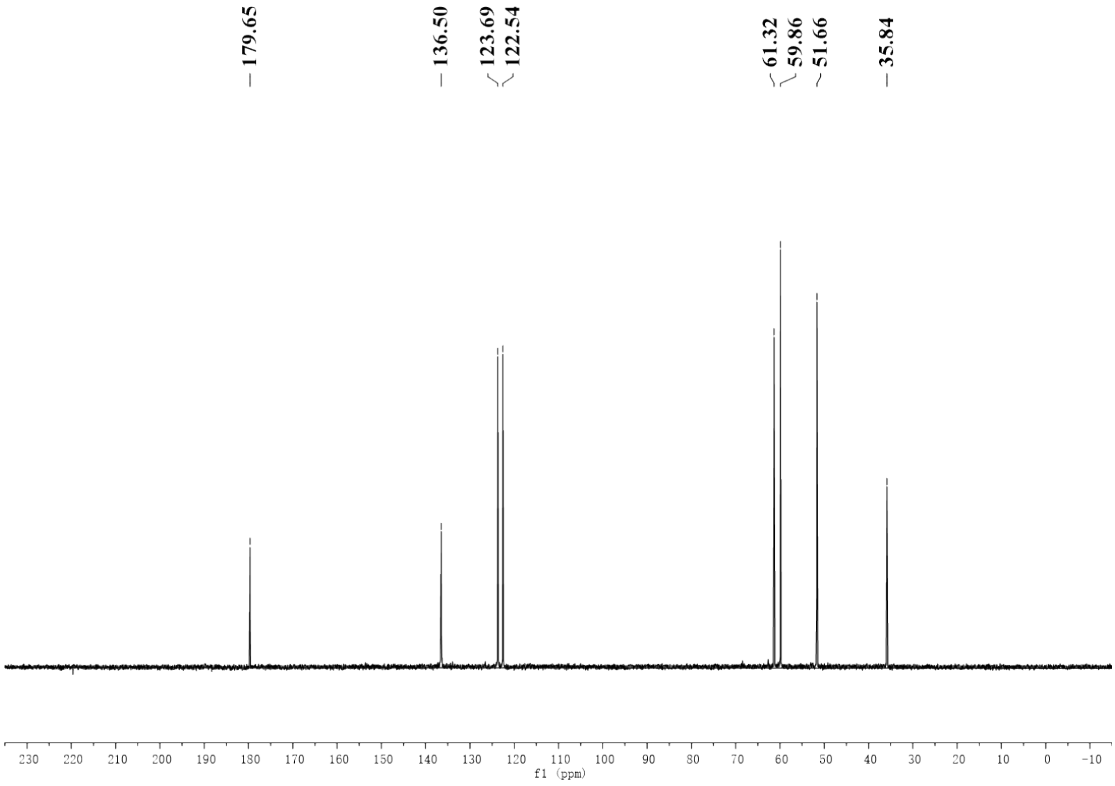


**Figure S5-2.** $^{13}$C NMR spectrum of IL **5.**

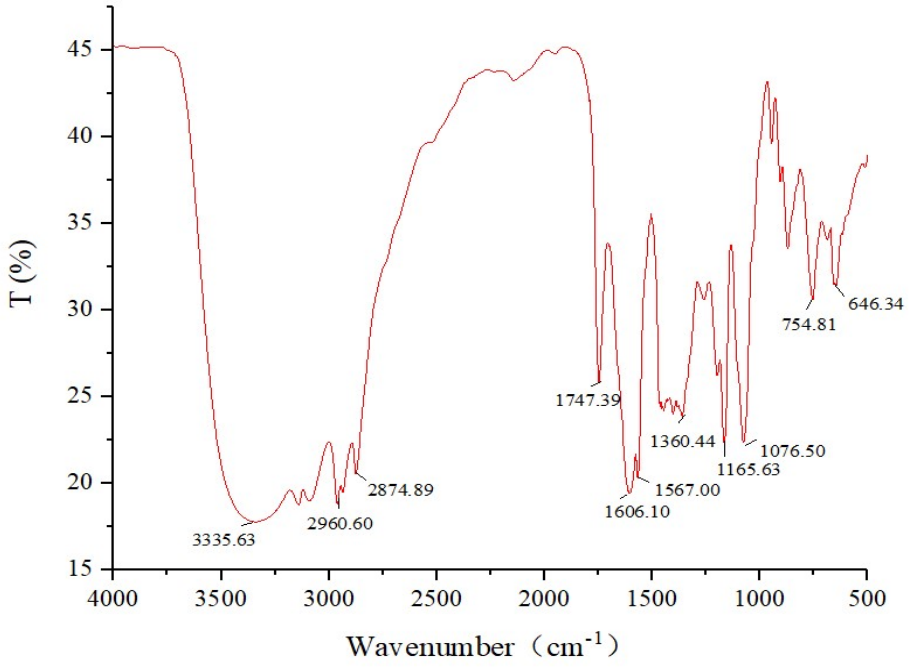


**Figure S5-3.** IR spectrum of IL **5.**

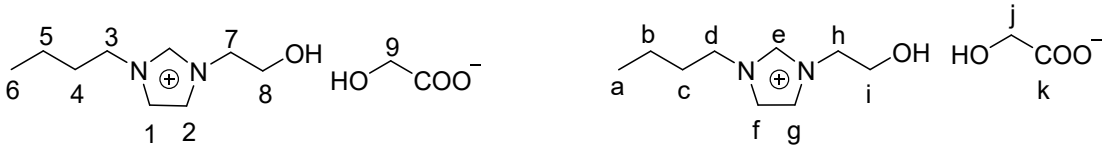


**Figure S6.** Distribution of $^{1}H$ NMR and $^{13}C$ NMR spectra of **1**.

**Table S1** $^{1}H$ NMR data of IL **1** in $D_2O$ (δ, ppm).

| H(1,2) | H(3,7) | H(4) | H(5) | H(6) | H(8) | H(9) |
|---|---|---|---|---|---|---|
| 7.49 (2H,s) | 3.89 (4H,s) | 1.82 (2H,m) | 1.29 (2H,m) | 0.89 (3H,t) | 4.18 (2H,t) | 4.28 (2H,m) |

$^{13}C$ NMR data of IL **1** in $D_2O$ (δ, ppm).

| $C^a$ | $C^b$ | $C^c$ | $C^d$ | $C^e$ | $C^f$ | $C^g$ | $C^h$ | $C^i$ | $C^j$ | $C^k$ |
|---|---|---|---|---|---|---|---|---|---|---|
| 12.84 | 18.91 | 31.36 | 49.45 | 135.57 | 122.61 | 122.49 | 51.66 | 59.84 | 61.38 | 179.49 |

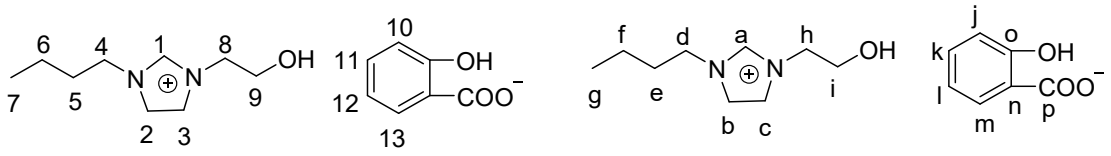

**Figure S7.** Distribution of $^{1}$H NMR and $^{13}$C NMR spectra of **2.**

**Table S2** $^{1}$H NMR data of IL **2** in $D_2O$ (δ, ppm).

| H(1) | H(2,3,10) | H(4) | H(5) | H(6) | H(7) | H(8) | H(9) | H(11,12) | H(13) |
|---|---|---|---|---|---|---|---|---|---|
| 8.69 | 7.39 | 3.88 | 1.75 | 1.23 | 0.85 | 4.08 | 4.22 | 6.88 | 7.74 |
| (1H,s) | (3H,m) | (2H,m) | (2H,m) | (2H,dd) | (3H,t) | (2H,t) | (2H,m) | (2H,m) | (1H,dd) |

$^{13}$C NMR data of IL **2** in $D_2O$ (δ, ppm).

| $C^a$ | $C^b$ | $C^c$ | $C^d$ | $C^e$ | $C^f$ | $C^g$ | $C^h$ | $C^i$ | $C^j$ | $C^k$ | $C^l$ | $C^m$ | $C^n$ | $C^o$ | $C^p$ |
|---|---|---|---|---|---|---|---|---|---|---|---|---|---|---|---|
| 135 | 121 | 122 | 49. | 31. | 18. | 12. | 51. | 59. | 116 | 133 | 117 | 130 | 118 | 160 | 174 |
| .09 | .99 | .36 | 12 | 01 | 77 | 67 | 49 | 58 | .12 | .72 | .47 | .34 | .88 | .06 | .21 |

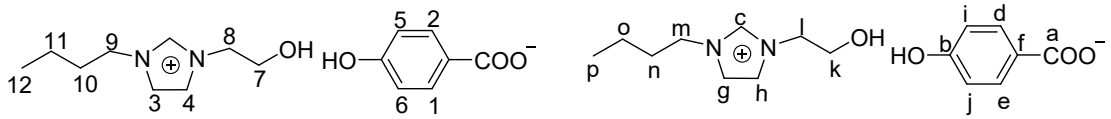

**Figure S8.** Distribution of $^{1}$H NMR and $^{13}$C NMR spectra of **3.**

**Table S3** $^{1}$H NMR data of IL **3** in $D_2O$ (δ, ppm).

| H(1,2) | H(3,4) | H(5,6) | H(7) | H(8) | H(9) | H(10) | H(11) | H(12) |
|---|---|---|---|---|---|---|---|---|
| 7.73 | 7.41 | 6.80 | 4.22 | 4.09 | 3.86 | 1.76 | 1.24 | 0.85 |
| (2H,d) | (2H,d) | (2H,d) | (2H,m) | (2H,t) | (2H,m) | (2H,m) | (2H,dd) | (3H,t) |

$^{13}$C NMR data of IL **3** in $D_2O$ (δ, ppm).

| $C^a$ | $C^b$ | $C^c$ | $C^d$ | $C^e$ | $C^f$ | $C^g$ | $C^h$ | $C^i$ | $C^j$ | $C^k$ | $C^l$ | $C^m$ | $C^n$ | $C^o$ | $C^p$ |
|---|---|---|---|---|---|---|---|---|---|---|---|---|---|---|---|
| 174 | 160 | 135 | 131 | 131 | 127 | 127 | 122 | 122 | 115 | 59. | 51. | 49. | 31. | 18. | 12. |
| .84 | .25 | .55 | .34 | .34 | .27 | .27 | .38 | .26 | .26 | 71 | 51 | 29 | 14 | 82 | 71 |

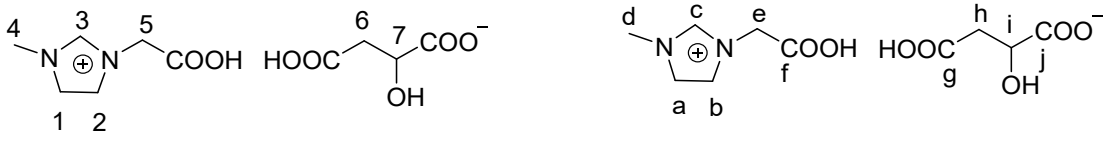

**Figure S9.** Distribution of $^{1}H$ NMR and $^{13}C$ NMR spectra of **4.**

## Table S4

$^{1}H$ NMR data of IL **4** in $D_2O$ (δ, ppm).

| H(1,2) | H(3) | H(4) | H(5) | H(6) | H(7) |
|---|---|---|---|---|---|
| 7.38 | 8.66 | 3.87 | 4.78 | 2.76 | 4.43 |
| (2H,s) | (1H,s) | (3H,s) | (2H,s) | (2H,dddd) | (1H,ddd) |

$^{13}C$ NMR data of IL **4** in $D_2O$ (δ, ppm).

| $C^a$ | $C^b$ | $C^c$ | $C^d$ | $C^e$ | $C^f$ | $C^j$ | $C^h$ | $C^i$ | $C^g$ |
|---|---|---|---|---|---|---|---|---|---|
| 123.42 | 123.27 | 136.99 | 67.49 | 51.69 | 175.04 | 177.50 | 39.09 | 36.81 | 172.10 |


**Figure S10.** Distribution of $^{1}H$ NMR and $^{13}C$ NMR spectra of **5.**

## Table S5

$^{1}H$ NMR data of IL **5** in $D_2O$ (δ, ppm).

| H(1) | H(2,3) | H(4) | H(5,6) | H(7) |
|---|---|---|---|---|
| 8.76 | 7.49 | 4.32 | 3.93 | 3.91 |
| (1H,s) | (2H,m) | (2H,m) | (4H,d) | (3H,s) |

$^{13}C$ NMR data of IL **5** in $D_2O$ (δ, ppm).

| $C^a$ | $C^b$ | $C^c$ | $C^d$ | $C^e$ | $C^f$ | $C^g$ | $C^h$ |
|---|---|---|---|---|---|---|---|
| 179.65 | 136.50 | 123.69 | 122.54 | 61.32 | 59.86 | 51.66 | 35.84 |

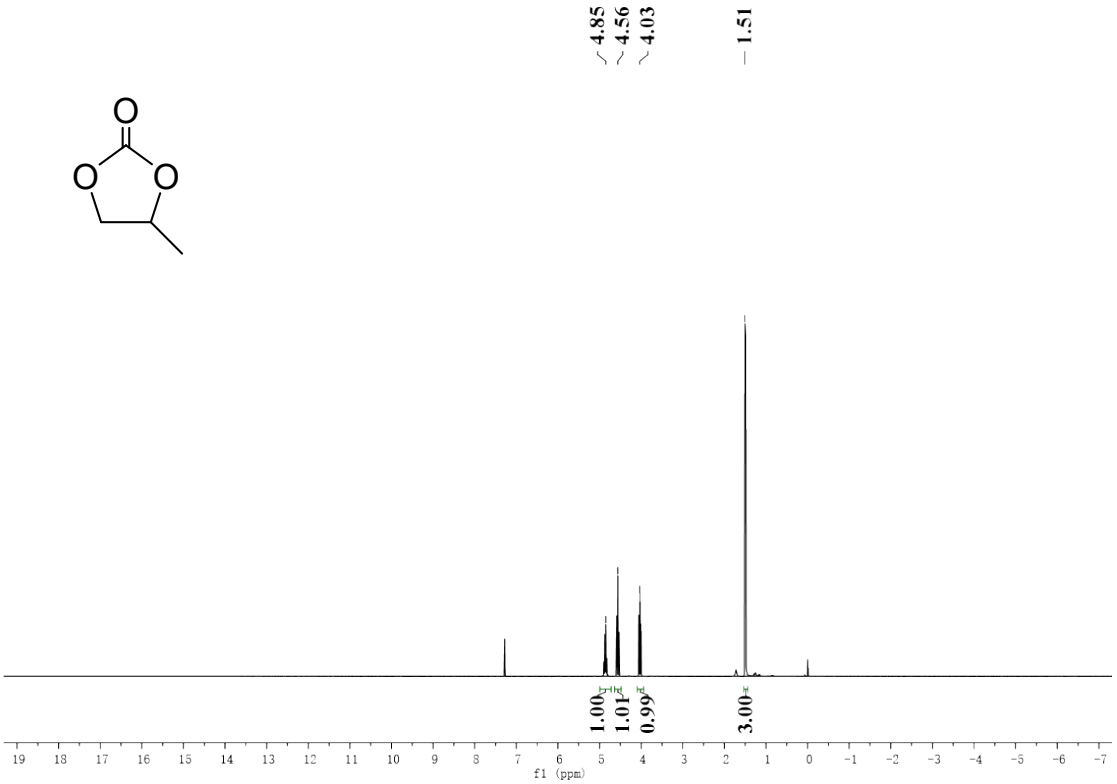


122

123 **Figure S11.** [1]H NMR spectrum of 4-methyl-1,3-dioxolan-2-one.

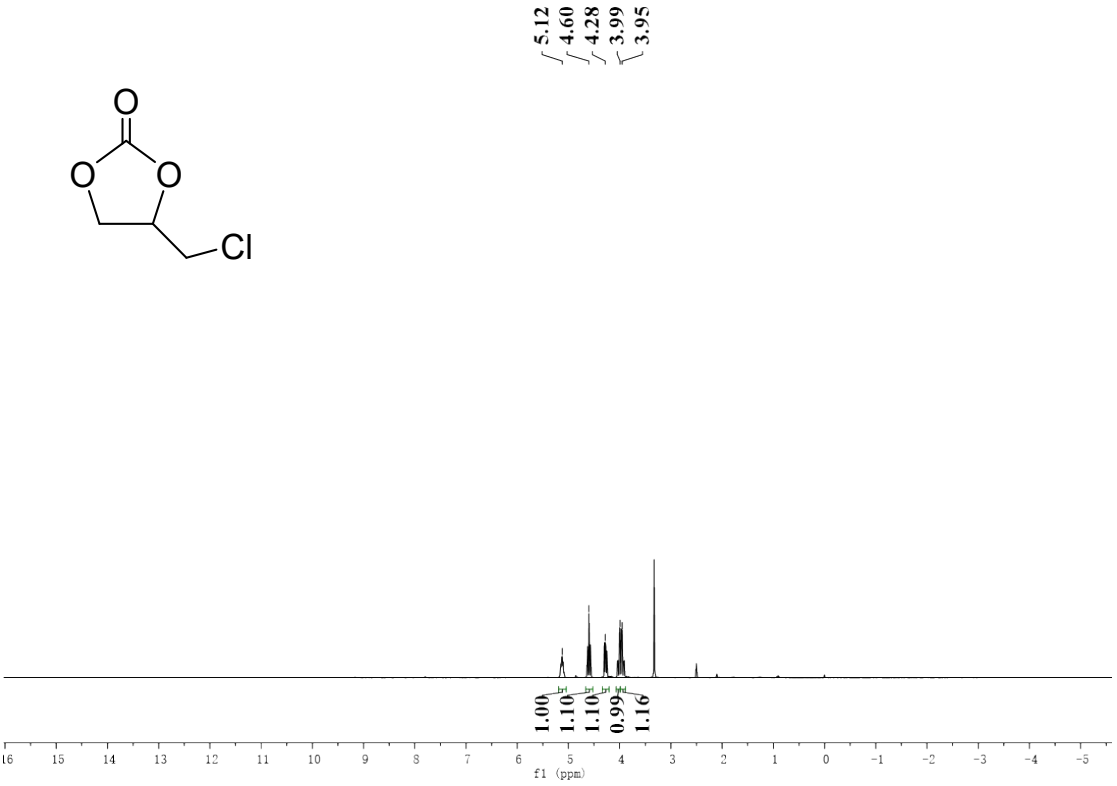


124

125 **Figure S12.** [1]H NMR spectrum of 4-(chloromethyl)-1,3-dioxolan-2-one.

126

127

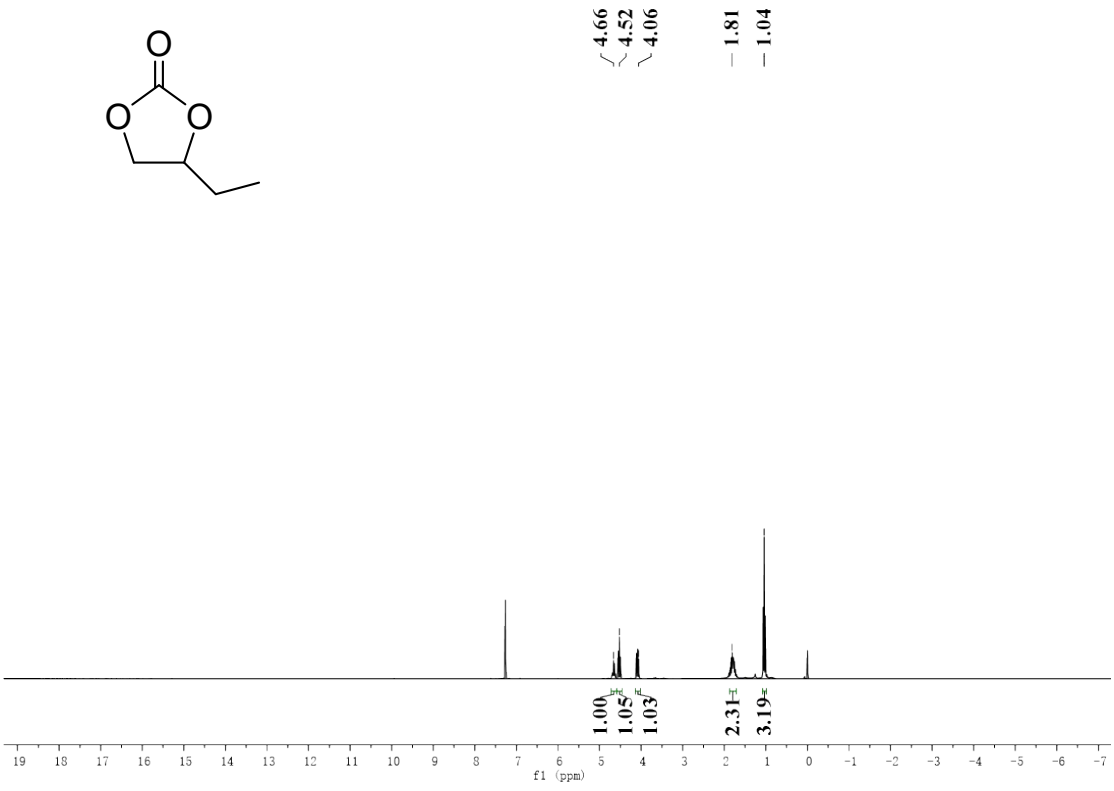


**Figure S13.** $^{1}$H NMR spectrum of 4-ethyl-1,3-dioxolan-2-one.

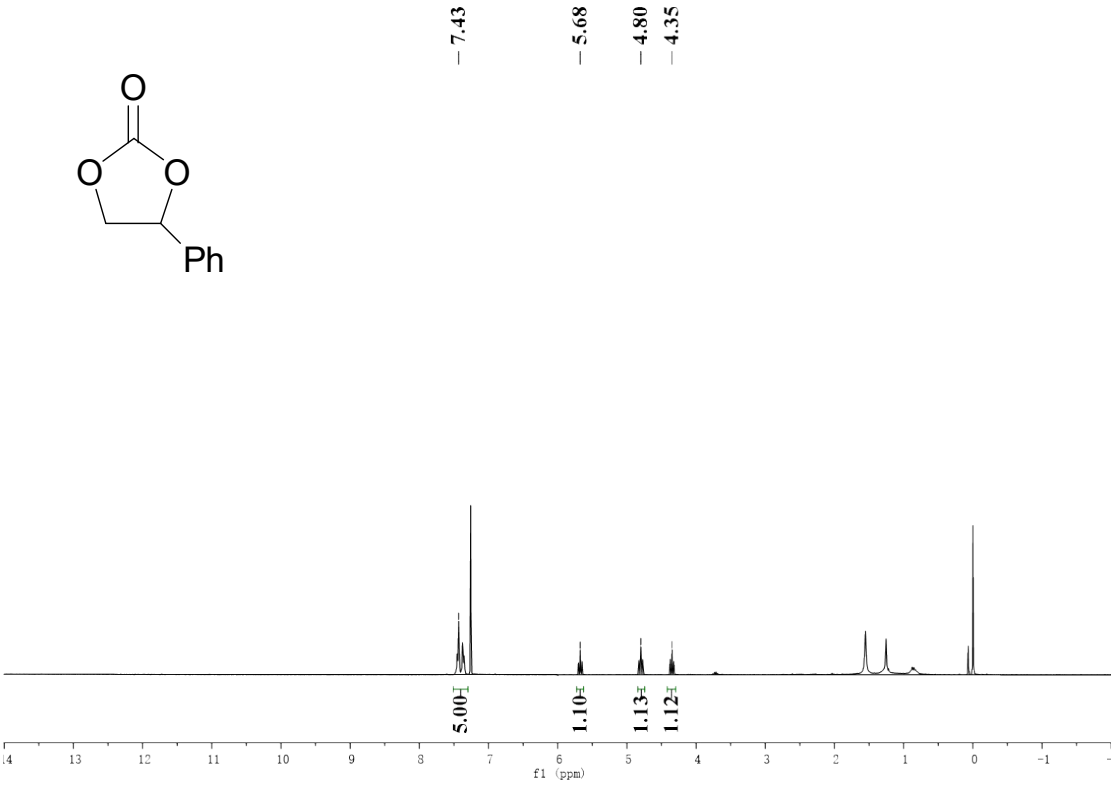


**Figure S14.** $^{1}$H NMR spectrum of 4-phenyl-1,3-dioxolan-2-one.

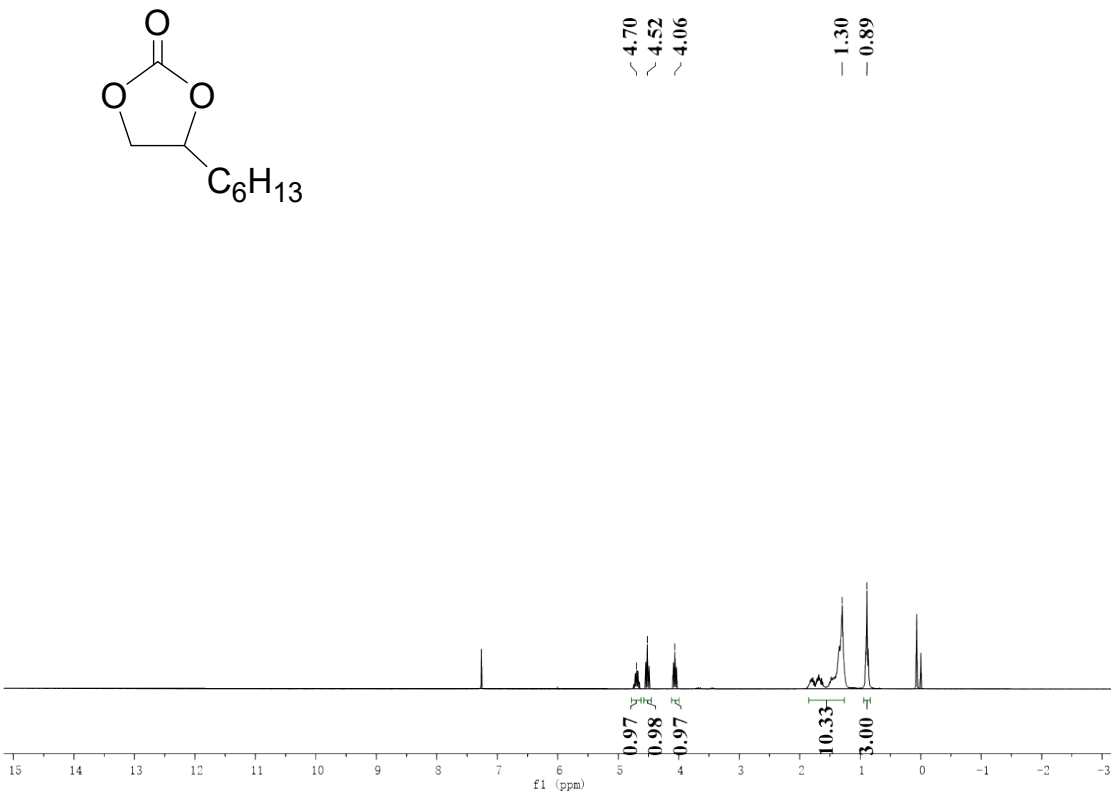


133

134 **Figure S15.** [1]H NMR spectrum of 4-Hexyl-1,3-dioxolan-2-one.

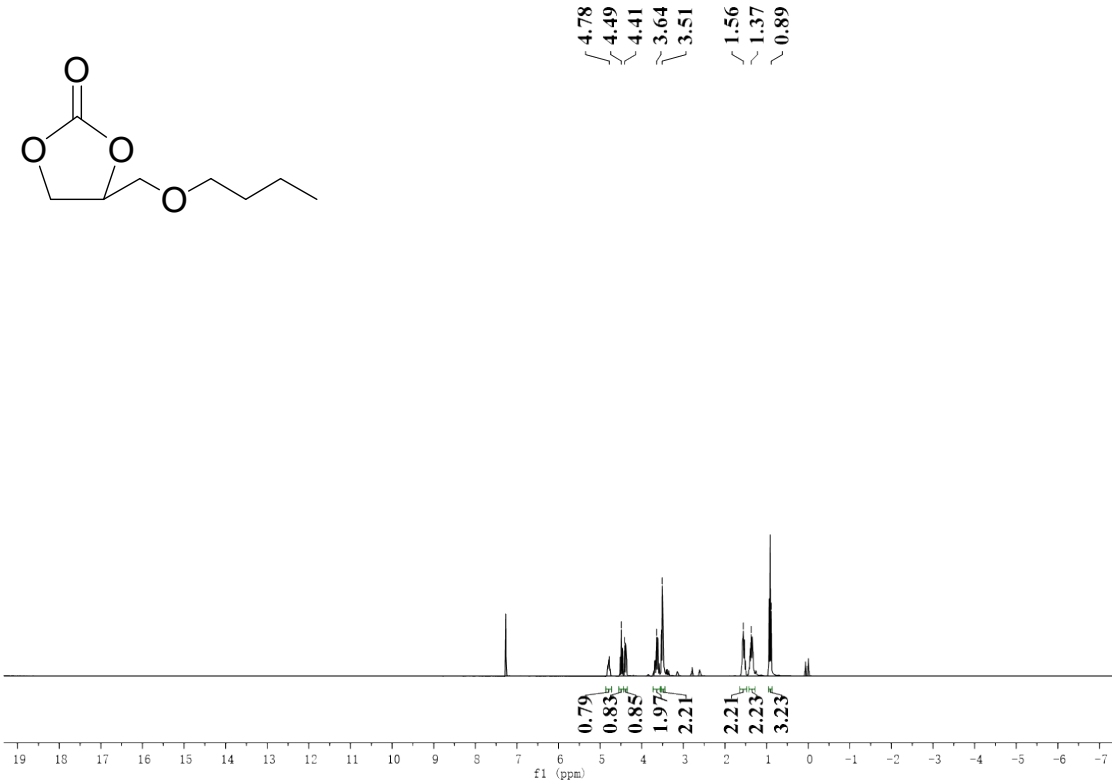


135

136 **Figure S16.** [1]H NMR spectrum of 4-butoxymethyl-1,3-dioxolan-2-one.

137

**Table S6.** Kinetic Equations and Kinetic Parameters at Different Temperature.

| T/(℃) | Kinetic equation | $R^2$ | $k$($min^{-1}$) | 1/T($k^{-1}$) | In $k$ |
|---|---|---|---|---|---|
| 85 | y=0.0015x-0.0079 | 0.9977 | 0.0015 | 0.00279 | -6.4890 |
| 90 | y=0.0019x-0.0083 | 0.9936 | 0.0019 | 0.00275 | -6.2554 |
| 95 | y=0.0024x-0.0172 | 0.9945 | 0.0024 | 0.00271 | -6.0075 |
| 100 | y=0.0028x-0.0012 | 0.9999 | 0.0028 | 0.00268 | -5.8674 |

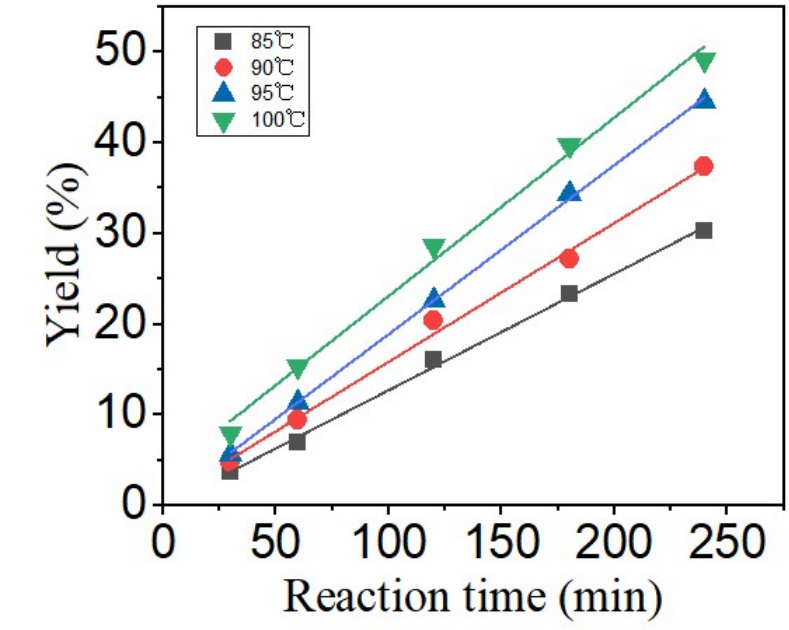


**Figure S17.** The chloropropene carbonate yield-time profile at different temperatures catalyzed by IL **1** as catalyst. Reaction conditions: n[epichlorohydrin] = 0.06383 mol, $CO_2$ 0.1 MPa, IL **1** 0.8 mol%.

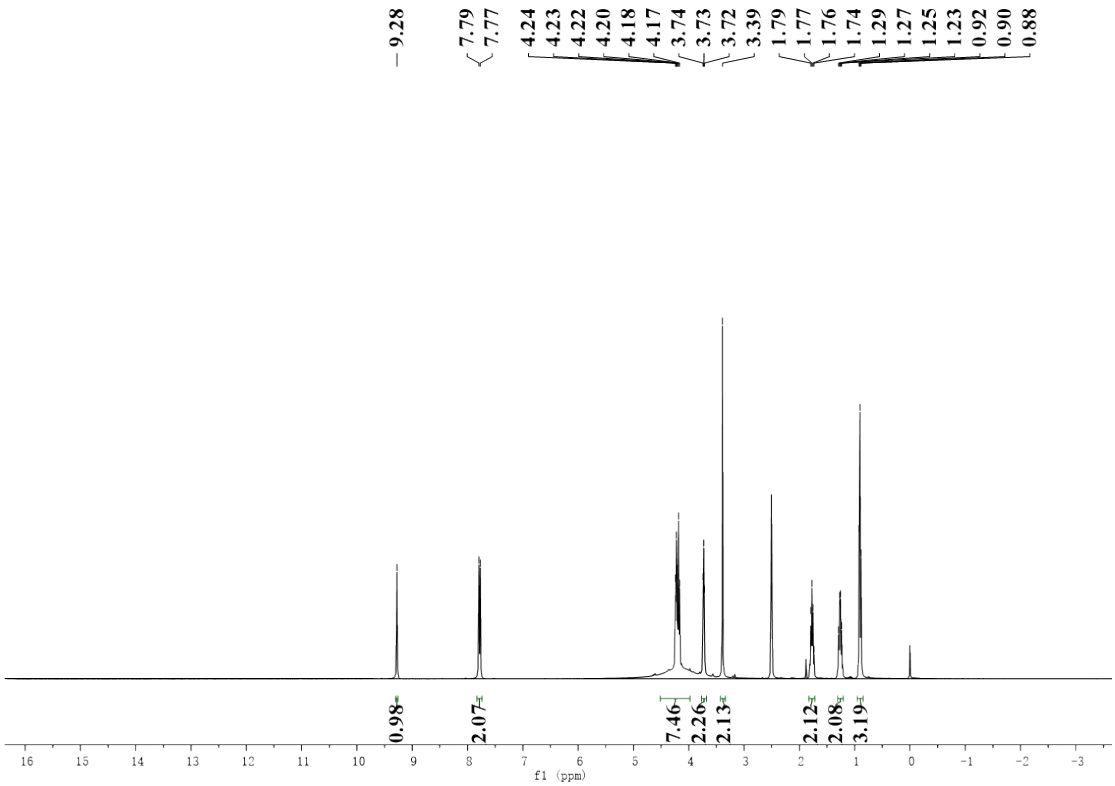


143

144

145 **Figure S18-1.** [1]H NMR spectrum of [HEBim][GA] in DMSO.

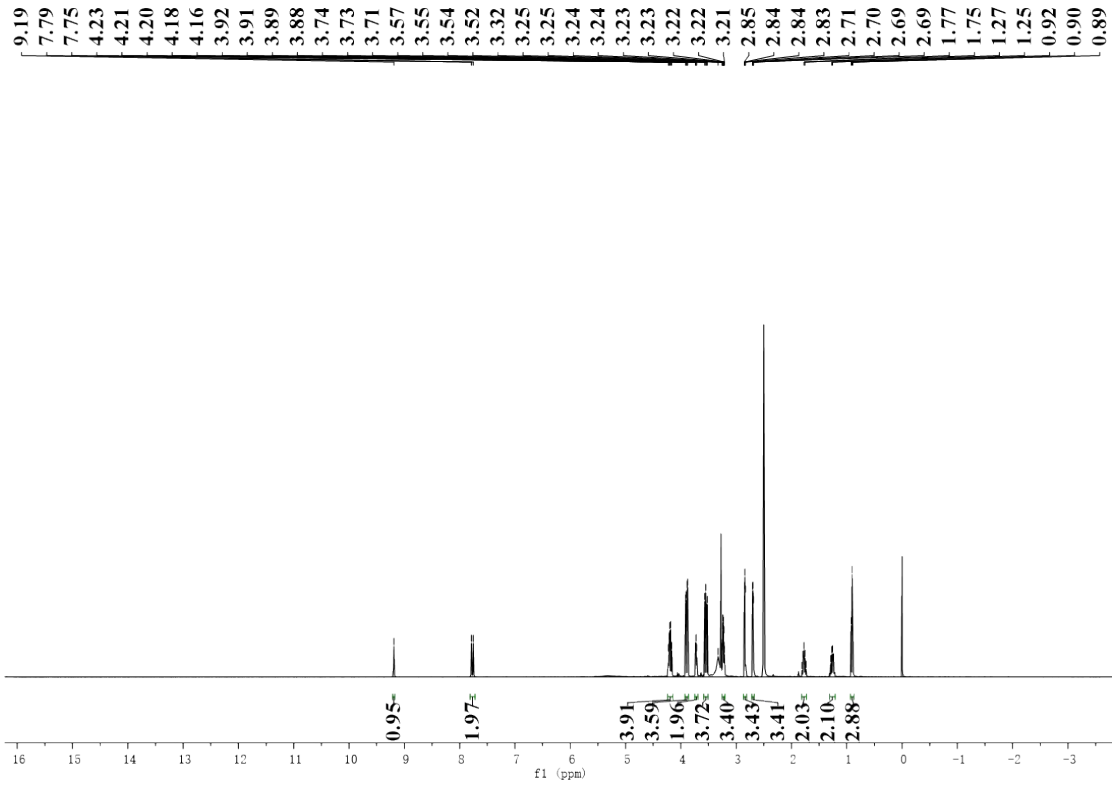


146

147 **Figure S18-2.** [1]H-NMR spectrum for [HEBim][GA] + epichlorohydrin at 30 °C and t = 0.5 h

148 in DMSO.

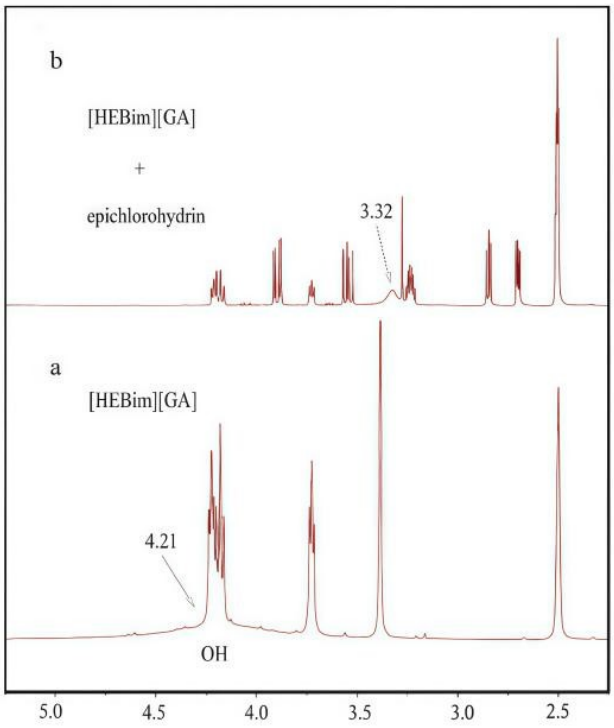


**Figure S19** (a)$^{1}$H-NMR spectrum for [HEBim][GA] in DMSO. (b) $^{1}$H-NMR spectrum for [HEBim][GA] epichlorohydrin at 30 °C and t = 0.5 h in DMSO.

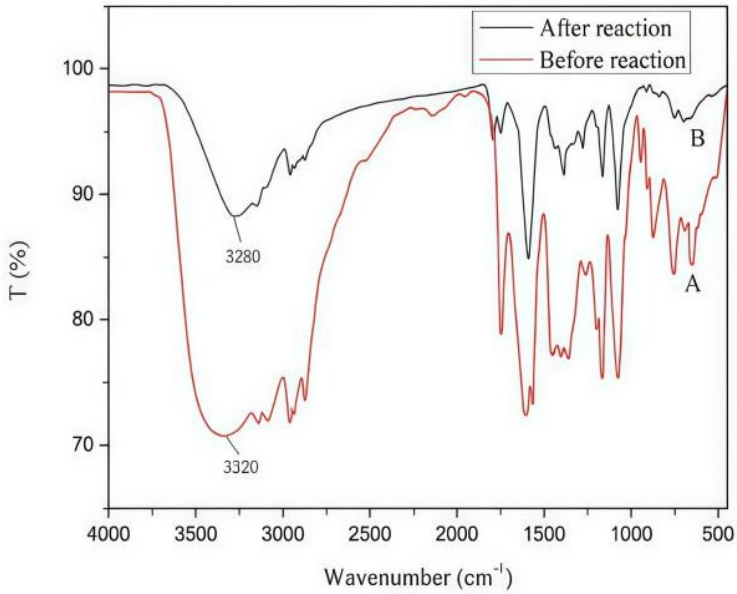


**Figure S20** FT-IR spectra of catalyst: A: Before reaction, B: After reaction.

**Kinetic Analysis of IL 1**

The synthesis of chloropropene carbonate was chosen as themodel to study the kinetics of the IL **1** reaction. According to the literature, the reaction kinetics of $CO_2$ in

chloropropylene carbonate is a first order reaction[1-4].

In the rate equation used to study the kinetics of the reaction between epichlorohydrin and $CO_2$. In order to determine the reaction order of the catalyst (IL **1**), four independent experiments were conducted under the optimal reaction conditions, where the reaction temperature was maintained at 95 °C, the initial $CO_2$ pressure was set at 0.1 MPa, and the reaction time was fixed at 0.5, 1, 2, 3, 4 h. In each experiment, the concentration of IL **1** was systematically varied. Specifically, the four distinct concentrations of IL **1** were set at 0.6 mol%, 0.7 mol%, 0.8 mol%, and 0.9 mol%, respectively. For each individual experiment, the designated amount of IL **1** catalyst and 63.83 mmol of epichlorohydrin were sequentially added into the reactor. Subsequently, the reactor was hermetically sealed. It was then immersed in an oil bath pre - heated to 95 °C, and $CO_2$ gas was introduced until the pressure inside the reactor reached 0.1 MPa. The magnetic stirrer was activated, and the reaction was allowed to proceed for a specified time Throughout the reaction process, the reaction system was monitored at regular intervals. The reaction mixture was analyzed at different time points to determine the yield of chloropropene carbonate. This approach enabled a comprehensive investigation of the impact of IL **1** concentration on the reaction kinetics and product yield under the established experimental reaction conditions.

At the same time, the reaction order of epoxide was studied by the same method. The amount of epichlorohydrin is designed to 80.00, 63.83, 46.00, 32.00 mmol, respectively.

**Determination of the Rate Constant**

Research shows the rate constant of a reaction is related to the rate constant. The higher the rate constant value indicates the faster reaction rate[5,6]. As such the reaction rate constants were investigated at four different temperatures(85 °C, 90 °C, 95 °C and 100 °C). Typically, epichlorohydrin (63.83 mmol) and IL **1** (0.8 mol%) were set into oil bath. Subsequently, the reactor was hermetically sealed. It was then immersed in an oil bath pre - heated to the corresponding temperature, and $CO_2$ gas was introduced until the pressure inside the reactor reached 0.1 MPa. The magnetic stirrer was activated, and the reaction was allowed to proceed. After reaching the expected time, the reaction was stopped. According to the Fig.8 and Figure S17, it can be found that $\ln[1/(1-\alpha)]$ has a linear fit with the reaction time. With the different rate constants of $k$, the slopes of the fitted curves conform to quasifirst-order kinetics.

## Notes and references


1. Y. Sang, Z. Shu, Y. Wang, L. Wang, D. Zhang, Q. Xiao, F. Zhou and J. Huang, *Applied Surface Science*, 2022, **585**, 152663-152671.
2. S. Li, Y. Liu, L. Shi, T. Hu, M. Li, C. Zhang, S. Shan and Y. Zhi, *Journal of Environmental Chemical Engineering*, 2024, **12**, 111989.
3. Y. Wu, A. Chen, X. Liu, J. Xu, Y. Wang, K. Mumford, G. W. Stevens and W. Fei, *Chemical Engineering and Processing - Process Intensification*, 2021, **159**, 108235-108241.
4. B. Zou, L. Hao, L. Y. Fan, Z. M. Gao, S. L. Chen, H. Li and C. W. Hu, *Journal of Catalysis*, 2015, **329**, 119-129.
5. M. Liu, B. Liu, S. Zhong, L. Shi, L. Liang and J. Sun, *Industrial & Engineering Chemistry Research*, 2015, **54**, 633-640.
6. C. Yang, Y. Chen, P. Xu, L. Yang, J. Zhang and J. Sun, *Molecular Catalysis*, 2020, **480**, 110637-110645.